2012

Comparison of Micro- and Nanoscale Fe+3-Containing (Hematite) Particles for their Toxicological Properties in Human Lung Cells In Vitro

Kunal Bhattacharya
Dublin Institute of Technology, kunal.bhattacharya@dit.ie

Eik Hoffmann
Institute of Hygiene and Occupational Medicine, University of Duisburg-Essen, Essen, Germany,

Roel Schins
Institut für Umweltmedizinische Forschung (IUF) an der Heinrich-Heine University Düsseldorf, Germany

Jens Boertz
Institute for Reference Materials and Measurements (IRMM), European Commission - Joint Research Centre, Geel, Belgium

Eva-Maria Prantl
Institute of Hygiene and Occupational Medicine, University of Duisburg-Essen, Essen, Germany,

See next page for additional authors

Authors
Kunal Bhattacharya, Eik Hoffmann, Roel Schins, Jens Boertz, Eva-Maria Prantl, Gerrit Alink, Hugh Byrne, Thomas Kuhlbusch, Qamar Rahman, Hartmut Wiggers, Christof Schulz, and Elke Dopp

Toxicological Sciences
(Accepted: November, 2011)
Final Submitted Format

Comparison of micro- and nanoscale Fe^{+3}-containing (hematite) particles for their toxicological properties in human lung cells *in vitro*

Kunal Bhattacharya[1,2], Eik Hoffmann[3], Roel Schins[4], Jens Boertz[5], Eva-Maria Prantl[1],Gerrit M. Alink[6], Hugh James Byrne[2], Thomas A.J. Kuhlbusch[7,8], Qamar Rahman[9], Hartmut Wiggers[8,10], Christof Schulz[8,10], Elke Dopp[1,8*]

[1]Institute of Hygiene and Occupational Medicine, University of Duisburg-Essen, Essen, Germany,
[2]Nanolab Research Centre, FOCAS Institute, Dublin Institute of Technology, Dublin, Ireland
[3]Institute of Biological Sciences, Cell Biology and Biosystems Technology, University of Rostock, Rostock, Germany
[4]Institut für Umweltmedizinische Forschung (IUF) an der Heinrich-Heine University Düsseldorf, Germany
[5]Institute for Reference Materials and Measurements (IRMM), European Commission - Joint Research Centre, Geel, Belgium
[6]Division of Toxicology, Wageningen University, The Netherlands
[7]Institute of Energy and Environmental Technology e.V., Duisburg, Germany
[8]CeNIDE, Center for Nanointegration, Duisburg-Essen, Duisburg, Germany
[9]Integral University, Lucknow, India
[10]IVG, Institute for Combustion and Gas dynamics, University of Duisburg-Essen Duisburg, Germany

*Corresponding author: Prof. Dr. Elke Dopp
Universität Duisburg-Essen
Institut für Hygiene und Arbeitsmedizin
Hufelandstraße 55
45122 Essen
GERMANY

Tel.: 0049 201/723 4578
Fax: 0049 201/723 4546
e-mail: elke.dopp@uni-due.de

Keywords: nanoscale particles, microscale particles, genotoxicity, cytotoxicity, radical formation

ABSTRACT:

The specific properties of nanoscale particles, large surface-to-mass ratio and highly reactive surfaces, have increased their commercial application in many fields. However, the same properties are also important for the interaction and bio-accumulation of the non-/biodegradable nanoscale particles in a biological system and are a cause for concern. Hematite (α-Fe_2O_3), being a mineral form of Fe(III) oxide, is one of the most used iron oxides besides magnetite. The aim of our study was the characterization and comparison of biophysical reactivity and toxicological effects of α-Fe_2O_3 nano- ($d < 100$ nm) and microscale ($d < 5$ µm) particles in human lung cells. Our study demonstrates that the surface reactivity of nanoscale α-Fe_2O_3 differs to that of microscale particles with respect to the state of agglomeration, radical formation potential, and cellular toxicity. The presence of proteins in culture medium and agglomeration were found to affect the catalytic properties of the hematite nano- and microscale particles. Both the nano- and microscale α-Fe_2O_3 particles were actively taken up by human lung cells *in vitro*, although, they were not found in the nuclei and mitochondria. Significant genotoxic effects were only found at very high particle concentrations (> 50 µg/ml). The nanoscale particles were slightly more potent in causing cyto- and genotoxicity as compared to their microscale counterparts. Both types of particles induced intracellular generation of reactive oxygen species. This study underlines that α-Fe_2O_3 nanoscale particles trigger different toxicological reaction pathways than microscale particles. However, the immediate environment of the particles (biomolecules, physiological properties of medium) modulates their toxicity on the basis of agglomeration rather than their actual size.

Introduction

The large surface-to-mass ratios and the reactive surfaces of nanoparticles are important for the interaction and bio-accumulation of the non-/biodegradable nanoscale particles in biological systems and in organisms. This raises concern of possible risks, now also seen and evaluated by international regulatory committees. In order to explore the possible health effects and regulate occupational and non-occupational exposure scenarios, the Organization for Economic Cooperation and Development (OECD) has generated a list of 14 commercially important nanoparticulate materials, which includes iron oxide [1]. In this context, it becomes important to determine the bio-nano-interaction of the iron oxide nanoscale particles following respiratory exposure. Hematite, being a mineral form of Fe(III) oxide, exists in several polymorphous subtypes (α-, γ-Fe_2O_3), has about 70% iron content and, due to its utilization as a pigment, is one of the most industrially used forms of iron oxide besides magnetite. The use of Fe_2O_3 nanoscale particles also includes drug targeting of cancer cells, tracking target cells using labeling, and imaging techniques like magnetic resonance tomography [2].

In vivo studies with Fe_2O_3 nanoscale particles have demonstrated severe inflammatory and toxicity responses in rats exposed to the nanoscale particles through inhalation [3, 4]. Fe_2O_3 particles (diameter < 100 nm) have been found to translocate and interact with the olfactory nerve and trigeminus of brain stem after 14 days post-inhalation in mice models [5]. Other studies have demonstrated that Fe_2O_3 nanoscale particles cause oxidative stress to human bronchoalveolar epithelial and murine neuronal cells leading to loss of cell viability, genotoxicity and causing a change in the electrical activity [6, 7]. In contrast to these finding, other studies performed with microscale and nanoparticulate Fe_2O_3 had described them both to be nontoxic under *in vitro* test conditions in human small airway epithelial and mouse fibroblast cells (exposure concentration up to 400 µg/cm²) [8]. Therefore, it is of interest to observe the difference in the bio-nano-interaction between Fe_2O_3 nano- and microscale particles in human lung cells *in vitro* and to correlate the effect with their physico-chemical properties.

Most studies under *in vitro*-conditions consider the basic physico-chemical characteristics of the nanoscale particles, such as shape, size and surface coating. However, recent studies have shown that the surface of the nanoscale particles changes after interaction with the surrounding environment through opsonization, solvation, protein corona formation and agglomeration [9, 10].

The present study characterizes the biophysical reactivity of Fe_2O_3 nano- (d < 100 nm) and microscale (d < 5 µm) particles under *in vitro* test conditions in human lung epithelial and fibroblast cells. Physico-chemical properties of Fe_2O_3 particles were determined through morphological investigations with scanning electron microscopy (SEM), specific surface analysis using Brunauer-Emmett-Teller (BET)

technique, determination of zeta potential and particle-size distribution via dynamic light scattering (DLS), and by the determination of total and leachable iron content and surface reactivity through electron paramagnetic resonance (EPR). The biological responses to the Fe_2O_3 nano- and microscale particles were studied by transmission electron microscopy (TEM), cyto- and genotoxicity analyses, measurement of intracellular reactive oxygen species (ROS) generation, and mitochondrial membrane potential detection. This study was designed to investigate the influence of particle size on biological effects in human lung cells after exposure. Additionally, the study explores the modification of the metal oxide (hematite) nanoscale particles in their immediate environment (media) in correlation to microscale particle with same chemical compositon.

Material and Methods

Nanoparticles and reagents

Hematite (α-Fe_2O_3) nano- (Cat. No. - 529311) and microscale (Cat. No. - 310050) particles were purchased from Sigma-Aldrich. According to the manufacturer's specifications, the average size range of the nanoscale particle was 10 - 100 nm and the microscale particle was 0.5 - 5 µm. Both the particles had a specified purity of $\geq$ 99.9% and an average molecular weight of 159.69 g/mol. Defined keratinocyte serum free medium (DKSFM) supplemented with 0.1% Epithelial Growth Factor (EGF) protein was purchased from GIBCO™ (Cat. No. - 10744). All the other supplements for cell culture media and required reagents were bought from Sigma-Aldrich, Germany. Fluorescent dyes, 2',7'-dichlorodihydrofluo-rescein diacetate (H_2DCFDA) (Cat. No.-D-399) and SYBR-Green nucleic acid stain (Cat. No. - S7585) were purchased from Invitrogen, Germany.

Physico-chemical characterization of the Fe_2O_3 nano- and microscale particles

a) Scanning Electron Microscopy (SEM)

For the analysis, both the nano- and microscale particles were dried in an oven overnight at 100ºC and layered onto a Formavar coated copper grid and gold palladium coated under low vacuum. SEM images of the dry particle samples were obtained at 30 kV under high vacuum condition, using a Zeiss LEO 1530 Gemini Field-emission SEM coupled with energy dispersive X-ray spectrometer. Particle size analysis from the SEM images was performed manually using Zeiss AxioVision LE software measuring the average diameter of 50 particles per SEM image.

b) Adsorption isotherm according to Brunauer-Emmett-Teller (BET)

BET surface areas (m^2/g) of the α-Fe_2O_3 nano- and microscale particles were measured using Micromeritics Gemini 2360 instrument (Micromeritics, Bedfordshire, UK). Both the nano- and microscale particles having equal mass (1 gram) were degassed at 300°C for 3 h under inert conditions and the surface area measured by nitrogen adsorption under isothermal conditions using BET technique.

c) Zeta potential and particle size distribution using dynamic light scattering

Zeta potential and particle size distribution measurements of the α-Fe_2O_3 nano- and microscale particles were studied in different liquid suspensions using Malvern's NanoZetasizer-ZS series. Both, the nano- and microscale particles of equal concentrations (100 µg/ml) were suspended in a) MilliQ water (collected at 18.2 MΩ·cm resistivity; Model: Simplicity, Millipore Ireland), b) BEAS-2B cell lysate protein solution (final conc.: 450 µg/ml) prepared following protocol of Bhattacharya et al. [6], and c) Defined keratinocyte serum free medium (DKSFM) supplemented with 0.1% epithelial growth factor (EGF) protein. All the particle suspensions were kept at room temperature (25 ºC) for 1 h and then suspended using an ultrasonic bath (ULTRAsonik™ Cleaner, Model 57X, Ney Dental Inc., USA) at 25 ºC for 5 min at 310 W, 47 kHz. Zeta potential measurement was measured following the Smoluchowski model [11]. Dynamic light scattering was used for the determining the particle size distribution (Number percentage: count of the size of each particle and calculation of the percentage of particles of any specific size category). All the measurements were taken at an ambient temperature of 25°C.

d) Non-/leachable Fe(III) content

Non-/leachable Fe(III) content of the α-Fe_2O_3 nano- and microscale particles were determined through the spectrometric 1,10 phenanthroline chloride assay following the previously described protocol [6]. Spectroscopic analysis was performed using Unicam UV/Visible Spectrometer (ATI Unicam, Germany). A standard curve to interpolate the quantity of Fe(III) was prepared using 1–6 mM concentrations of $FeCl_3.6H_2O$ (Regression coefficient (R^2): 0.998).

e) Electron Spin Resonance (ESR) spectrometry

Surface reactivity of the nano- and microscale particles in acellular environment leading to the generation of $OH^{\bullet}$ radicals was studied using a spin trap, 5, 5-dimethyl-1-pyrroline-N-oxide (DMPO) and ESR spectrometry [6]. For the study, nano- and microscale α-Fe_2O_3 particles (Conc. - 125 µg/ml) were suspended in 1 ml ddH_2O and tested in the presence 120 mM H_2O_2 and 50 µl of 1 M DMPO. As a negative control, ddH_2O without particles was used. Generation of $OH^{\bullet}$ by the α-Fe_2O_3 nano- and microscale particles after treatment with SV-40 virus transformed with human bronchial epithelial (BEAS-2B) cell lysate followed by 120 mM H_2O_2 and 50 µl of 1 M DMPO was measured using technique as has been previously described [6].

All suspensions were incubated at 37°C for 2 h and filtered through a 0.45 µm syringe filter. The filtrates were immediately transferred to a glass capillary and measured using Miniscope MS200 EPR spectrometer at room temperature and the instrument settings as follows: magnetic field 3360 G, sweep width 100 G, scan time 30 sec, modulation amplitude 1975 G, receiver gain 1000. Quantification was done by accumulation of three different spectra each averaging three different scans. The amplitudes of all four peaks were taken and the outcomes were expressed as (ESR units in) arbitrary units (a.u.).

Biological interaction between α-Fe_2O_3 particles and human bronchial epithelial cells

a) Cell culture

SV40-transformed human bronchial epithelial (BEAS-2B) cells were obtained from the European collection of cell cultures (Cat. No.- 95102433) and were cultivated in defined keratinocyte serum free media (DKSFM) supplemented with 0.1% epithelial growth factor proteins and 1% antibiotics. The cells were cultivated at 36 ºC and 5% CO_2.

Human lung fibroblasts (IMR-90) were obtained from the American type culture collection (ATCC, CCL-186) and were cultivated in Roswell Park Memorial Institute medium (RPMI-1640) supplemented with 2 mM Glutamine, 1% non-essential amino acids (NEAA) and 5 % foetal bovine serum (FBS). The cells were cultivated at 36 ºC and 5% CO_2.

b) Transmission Electron Microscopy (TEM)

For the study, $10x10^5$ BEAS-2B cells were plated in a Falcon‘s T-75 flask and preincubated before exposure. Before exposure, α-Fe_2O_3 nano- and microscale particles (concentration: 50 µg/ml) were prepared and cells were exposed for 48 h. Post-exposure, the cells were washed with phosphate buffered saline solution (PBS) and fixed in 4% paraformaldehyde (EM grade; EMS, USA) and 0.1 % glutaraldehyde (EM grade; EMS, USA) in 0.1 M PHEM buffer (pH 6.9) for 45 min at room temperature followed by 3 h fixation in 4 % paraformaldehyde alone. Free aldehyde groups were neutralized by 50 mM glycine in 0.1 M PHEM. Cells were released from the plastic surface with a Teflon edge in PBS containing 1 % gelatin and centrifuged. Pellets were resuspended and pelleted in 10 % gelatin and incubated on ice. Gelatin-embedded pellets

were cut into square blocks and infiltrated in 2.3 M sucrose in PBS at 4 °C overnight and mounted onto copper pins afterwards. Samples were shock frozen in liquid nitrogen and then trimmed and cut with an Ultracut UCT cryotome (Leica, Germany) using a Cryotrim 45° diamond knife (Diatome, USA). Ultra-thin sections of 65 nm thickness were cut using a diamond knife at -120 °C, picked in 2 % methyl cellulose / 2.3 M sucrose and then placed on formvar coated grids. Cryosections were finally contrasted and sealed in 3 % uranyl acetate / 2 % methyl cellulose (1.5 parts / 8.5 parts). Several cryosections were analyzed and eight images per sample were taken using a Zeiss EM10 electron microscope.

c) Cell viability analysis

The study was performed using the Trypan blue assay. In brief, for each measurement, $1x10^5$ BEAS-2B and IMR-90 cells were plated individually in Falcon's T-25 flasks and pre-incubated for 24 h. For exposure, the α-Fe_2O_3 nano- and microscale particles were freshly suspended in DKSFM supplemented with 0.1% epithelial growth factor protein for BEAS-2B cells and in RPMI-1640 supplemented with 2 mM Glutamine, 1% non-essential amino acids (NEAA) and 5 % foetal bovine serum (FBS) for IMR-90 cells, at concentrations of 10, 25, 50, and 250 µg/ml. The cells were exposed for a time period of 24 h. For negative control cells were exposed to normal cell culture medium. In the BEAS-2B cells, 10 µM cis-diamminedichloroplatinum(II) (Cisplatin) exposure was used as a positive control [12]. For detecting the cell death percentage, the cells were washed twice with 2 ml of pre-warmed PBS, trypsinized and exposed to 0.5% Trypan blue solution. The cells were incubated for 4 min at 37 °C and viable (white) and dead (blue) cells were counted manually using a haemocytometer. The mean cell death percentage and cell viability percentage were calculated, setting negative controls at '0' and '100' percents, respectively. All the experiments were conducted in triplicates and statistically analyzed using one way ANOVA (exposure vs. negative control) followed by Holm-Sidak post-hoc test.

d) Genotoxicity analysis

Genotoxic effect of the α-Fe_2O_3 nano- and microscale particles was determined by analyzing DNA fragmentation using the alkaline comet assay technique (pH 12.7). For each measurement, $1x10^5$ cells (BEAS-2B) were plated individually in Falcon's T-25 flasks and pre-incubated for 24 h. The cells were exposed to a freshly prepared suspension of α-Fe_2O_3 nano- and microscale

particles at the concentrations of 10, 25, 50 and 250 µg/ml and for a time period of 24 h. As a negative control cells were treated with normal cell culture media (DKSFM supplemented with 0.1% epithelial growth factor protein) and as a positive control 200 µM N-ethyl-N-nitrosourea (ENU) was used to form alkylating adducts [13]. Post-exposure, the cells were washed, trypsinized and suspended in low melting agarose and cast onto a gel bond film. Following the polymerization of the agarose, the cells were lysed overnight in a freshly prepared and pre-cooled cell lysis buffer. Electrophoresis of the lysed cells was performed at a pH of 12.7 for 10 mins (conditions: 300 mA, 1.5 V/cm at 4°C), following which the agarose was treated with neutralization solution for 30 min and dehydrated in absolute CH_3COOH for 2 h. These agarose gels were dried in darkness overnight at 4°C and stained with SYBR-Green nucleic acid stain. Imaging and analysis were performed on a Leica upright microscope attached with a CCD camera and using 'Comet Assay IV' software (Perceptive Instruments, UK). The parameter of olive tail moment (OTM) was used for analysis of the DNA damage. The quantitative measurement of all the assays was expressed as mean percentage increase relative to unexposed control ± SD. Negative control values were set at '0'. The results were statistically analyzed (exposure vs. negative control) using one way ANOVA followed by Holm-Sidak post-hoc test.

e) Detection of intracellular reactive oxygen species (ROS)

Intracellular ROS were measured through spectroscopic analysis of fluorescent 2',7'-dichlorodihydrofluorescein diacetate (H_2DCFDA) dye. BEAS-2B cells at the concentration of $1x10^5$ cells per well were plated in 96 well plates and pre-incubated overnight. α-Fe_2O_3 nano- and microscale particles were freshly suspended in DKSFM media supplemented with 0.1% epithelial growth factor protein. BEAS-2B cells were exposed to α-Fe_2O_3 nano- and microscale particles at concentrations of 5, 10, and 50 µg/ml for 6, 12, and 24 h. As negative control, cells were treated with normal cell culture medium, while Cisplatin (10 µM) was used as positive control [14]. At the end of the exposure time, the cells were washed with PBS and exposed to H_2DCFDA dye at a concentration of 10 µM for 20 min. After staining, the cells were washed and re-suspended in PBS and the fluorescence at 535 nm was measured with excitation at 485 nm on a Tecan multiplate reader.

The metal chelator desferrioxamine mesylate (conc. 100 µM) was given to the BEAS-2B cells simultaneously with 5, 10 and 50 µg/ml Fe_2O_3 nano- and microscale particles for time periods of

12 and 24 h. After the lapse of the exposure time, the cells were washed and treated with the H_2DCFDA dye as previously described and the quantity of ROS was measured using the Tecan multiplate reader.

f) Detection of mitochondrial membrane potential

BEAS-2B cells at the concentration of $1x10^5$ cells per well were plated in 96 well plates and pre-incubated overnight. α-Fe_2O_3 nano- and microscale particles were freshly suspended in DKSFM media supplemented with 0.1% epithelial growth factor protein. BEAS-2B cells were exposed to Fe_2O_3 nano- and microscale particle at the concentrations of 5, 10, and 50 µg/ml for the time periods of 6, 12, and 24 h. As negative control cell were only treated with normal cell culture medium, while as a positive control 100 µM of ionophore Valinomycin was used. Post-exposure, the cells were washed thoroughly using PBS and exposed to 5 µM Rhodamine-123 dye. The cells were again incubated for 30 mins and then washed with PBS to remove excess dye. Measurements were obtained immediately at excitation and emission wavelengths of 488 and 535 nm using Tecan microplate reader.

The quantitative measurement of all the assays was expressed as mean percentage increase relative to unexposed control ± SD. Control values were set at 0%. Results were statistically analyzed using one way ANOVA followed by Holm-Sidak post-hoc test.

Results

Physico-chemical analysis of the α-Fe_2O_3 nano- and microscale particles

Scanning electron microscopic (SEM) images showed the α-Fe_2O_3 nano- and microscale particles to be heterogeneous in shape and size (Figure 1). Particle size distribution measured manually using Zeiss AxioVision LE software on the acquired SEM images, showed the percentage of nanoscale particles in the diameter range of <25 - 50 nm: 95%, >50 - 100 nm: 4% and >100 nm: 1%. Similarly, the percentage of microscale particles was found in the diameter range of ≤500 nm: 98% and >500 nm - 1.0 µm: 2%. Energy dispersive X-Ray spectroscopy showed the surface elemental composition of the α-Fe_2O_3 nano- and microscale particles to be 78.7% Iron (Fe) and 21.3% Oxygen (O).

Brunauer-Emmett-Teller (BET) surface area measurement of the dry α-Fe_2O_3 nano- and microscale particles of equal mass (1 g) revealed a surface area of 34.4 ± 0.2 m^2/g for the nanoscale and a surface area of 0.72 ± 0.1 m^2/g for the microscale particles. Based on surface area of a sphere (A) equation $A= \pi D^2$, (D= diameter of the sphere) the diameter of the nanoscale particles was 7 times smaller as compared to the microscale particles, keeping the mass constant. This fold difference in the BET surface area provided evidence that the nanoscale particles under dry condition were loosely bound single entities providing higher surface area for the nitrogen to be adsorbed and proved the accuracy of the particle size distribution analysis determined from the SEM images.

Zeta potential, particle size distribution (Number %; hydrodynamic diameter in nm) and polydispersity index of both the α-Fe_2O_3 nano- and microscale particles in suspension are shown in Table 1. Zeta potential charge measurement of the α-Fe_2O_3 nanoscale particles suspended in different liquid suspensions showed a decrease in their negative zeta potential towards neutral charge based on the ionic and biomolecular constitution of the liquid media (MilliQ water> cell lysate protein> DKSFM + 0.1% EGF) (Table 1). However, particle size distribution and polydispersity index measurements of the nanoscale particles suspended in MilliQ water and DKSFM supplemented with epithelial growth factor protein showed insignificant changes. Nanoscale particles suspended in cell lysate (native cellular) protein solution showed significant reduction in the particle size distribution indicating a reduction in the agglomeration of the

particles following interaction with the cellular proteins. The polydispersity index (≤1.0) indicated an instability of the particle suspension.

Suspension of the α-Fe_2O_3 microscale particles in different media showed a change in the zeta potential charge, similar to the nanoscale particles. Native cellular proteins were found to increase the negative zeta potential charge on the surface of the microscale particles (-30 ± 0.5 mV) (Table 1). Measurement of the particle size distribution of the microscale particles showed negligible differences when suspended in MilliQ and DKSFM supplemented with epithelial growth factor proteins and a significant reduction when suspended in cell lysate solution, similar to that observed with the nanoscale particles. Polydispersity index of all the microscale particle suspensions indicated a highly unstable particle suspension.

Presence of a higher zeta potential charge on the surface of the nanoscale particle as compared to the microscale particles when suspended in the MilliQ water proved a link between the particle surface charge and dimension. However, in suspensions containing inorganic ions and biomolecules, the nano- and microscale particles lost their dimensional specificity through reduction in equal zeta potential following adsorption and opsonization on the surface of the particles and their agglomeration. Agglomerates formed by nanoscale particles were found to be larger as compared to those formed by the microscale particles.

Spectroscopic analysis of leachable and non-leachable Fe(III) using 1, 10 phenanthroline chloride dye, showed a variation of 0.6 mM in the concentration of non-leachable Fe(III) between the nanoscale (5.2 mM) and microscale (5.8 mM) particles of equal mass (Figure 2A). The concentration of leachable Fe(III) on the surface of the α-Fe_2O_3 nanoscale particles was observed to be 7.5 times higher as compared to the microscale particles, indicating its dependence upon the available surface area (BET surface area) of the nano- and microscale particles (Figure. 2B).

Acellular hydroxyl radical ($OH^{\bullet}$) generation capability of the α-Fe_2O_3 nano- and microscale particles through the dissociation of hydrogen peroxide (H_2O_2) was studied using electron spin resonance (ESR) spectrometry. The results indicated 11 times higher formation of $OH^{\bullet}$ on the surface of the microscale particles (2,800 ± 450.0 ESR units) as compared to the nanoscale particles (252.3 ± 0.0 ESR units) when suspended for 2 h in MilliQ water with 120 mM H_2O_2

(Figure 3A and B). However, treatment of the nano- and microscale particles with cell lysate proteins resulted in 8 and 31 times higher generation of $OH^{\bullet}$ radicals by the nanoscale particles compared to the microscale particles at the time period of 4 and 6 h (Figure 3).

Biological interaction between α-Fe_2O_3 nano- or microparticles and human lung cell lines

Transmission electron microscopic (TEM) images of the interaction between the α-Fe_2O_3 nano- and microparticle and the BEAS-2B cells showed both types of particles intracellularly in close proximity to mitochondria (Fig. 5A and B). This indicates the possibility of direct or indirect stimulation of cell signaling leading to active mitochondrial involvement in oxidative stress. Neither nano- nor microscale particles were found within the nuclei and mitochondria in all examined samples. Although we did not carry out a quantitative analysis by stereological approaches, our TEM images provided evidence of an intracellular presence of nano- and microscale particles in agglomerates, which could induce oxidative stress and altered cell viability.

Exposure of BEAS-2B cells to the different concentrations of nano- and microscale particles resulted in a cytotoxic response reaching the maximum at the concentration of 250 µg/ml (Figure 5).

To compare the cell type specific response, human lung fibroblasts (IMR90, non-transformed) as well as human lung epithelial cells (BEAS-2B, SV40-virustransformed) were used for the experiments. IMR-90 cells exposed to the Fe_2O_3 nanoscale particles resulted in an increased loss of cell viability depending upon exposure concentration (Fig. 6A). EC_{50} was calculated and found to be at 148 µg/ml for nanoscale particles. The highest cytotoxicity was achieved at 250 µg/ml (40.18 ± 0.25%; p value $\leq$0.001). Reductions of cell viability at all the exposure concentrations measured were found to be statistically significant as compared to the negative control (Fig. 6A). BEAS-2B cells exposed to the α-Fe_2O_3 nanoscale particles resulted in a gradual loss of cell viability (Fig. 6B). The results show clearly that cyto- and genotoxicity caused by nano- and microscale particles can only be observed at very high concentrations of $\geq$ 50 µg/ml. At occupationally relevant concentrations of <10 µg/ml no cyto- and genotoxic effects can be observed (data not shown).

Generation of intracellular reactive oxygen species (ROS) in BEAS-2B cells exposed to Fe_2O_3 nanoscale particles was detected after 12 h of exposure and continued till later time points (Figure 7A). In contrast, exposure of the BEAS-2B cells to Fe_2O_3 microscale particles resulted in a generation of intracellular ROS after 6 h already (Figure 7B). Simultaneous exposure of the BEAS-2B cells to metal chelator (Desferrioxamine) and α-Fe_2O_3 nano- or microscale particles showed a time- and concentration-dependent generation of ROS. Desferrioxamine was able to bind Fe(III) ions at the shorter exposure time of 12 h and therefore, free radical production was reduced (Fig. 7 A and B).

Mitochondrial membrane potential measurements indicated a high metabolic activity at the measured time periods of 12 and 24 h post-exposure to the α-Fe_2O_3 nano- and microscale particles (Figure 8). While the initial measured response of the BEAS-2B cells showed the α-Fe_2O_3 nanoscale particles to cause higher mitochondrial activity at the time period of 12 h, as compared to the microscale particles, by 24 h it became equal for both types of particles. Valinomycin, a potential K^+ ionophore, was used as positive control in our study.

Discussion

To elucidate the interaction of particles with cellular systems, it is important to characterize and relate the physico-chemical properties of the particles under test conditions to their effect on cellular activity [15]. Our study showed that the surface of both α-Fe_2O_3 nano- and microscale particles has a significant interaction with the surrounding environment and alters the physical properties of the particles, depending upon the presence of ionic (salt) and biomolecules in their vicinity. Proteins were found to play an important role in agglomeration activity of both particle types. Particles suspended in native cellular protein fractions showed the highest agglomeration capacity compared to cell culture medium (DKSFM + 0.1% EGF) and water. Agglomeration of nanoparticles was higher compared to microparticles probably because of stronger van-der-Waals-forces. A modification of the composition or the chemical properties (e.g. the pH) of the surrounding medium resulted in changed agglomeration capacities of the particles. These findings are in agreement with studies of Kumar et al. [2] who found that the adsorption of biomolecules on the surface of particles followed by modification of the zeta potential and the agglomerate size play a vital role in their reactivity to the surrounding environment. Some key proteins such as albumin, immunoglobulin, fibrinogen, and apolipoproteins have been reported to bind strongly with iron oxide particles [2]. The formation of a protein corona has been suggested by several groups [9, 10,16,17].

Although the agglomeration capacity of the nanoparticles was higher compared to the microparticles, the available surface area of nanoparticles was greater than that of the microparticles. This might have influenced the leachable Fe(III) ion content which was higher in NP suspensions than in microparticle suspension. However, the differences in particle size, leachable Fe(III) and biological effects of nano- and microscale particles were reduced because of the agglomeration of particles in the cellular system.

All the mentioned physico-chemical parameters have an impact on toxicological effects in human cells like cellular uptake of particles, cyto-/genotoxicity, radical generation and changes in mitochondrial potential. The catalytic effect of α-Fe_2O_3 nano- and microparticles on the reduction of hydrogen peroxide (H_2O_2) indicated a reactive surface capable of generating extracellular reactive oxygen species and causing oxidative stress in the cells. Both the α-Fe_2O_3 nano- and microscale particles were found to generate acellular ROS depending upon their

particle size distribution, their agglomeration in suspension with/without proteins and the presence of hydrogen peroxide. Fe(III) has been stated to catalyze the reduction of H_2O_2 to hydroperoxyl ($OOH^{\bullet}$) and hydroxyl ($OH^{\bullet}$) radicals [18,19]. Native cellular proteins were seen to reduce the particle size distribution of the α-Fe_2O_3 nanoscale particles through surface interaction leading to higher levels of ROS generation as compared to the microscale particles.

Insignificant changes in the pH of the cell culture medium indicated the short duration of generated free radicals on the surface of the particles. Treatment of particles with L-ascorbic acid and whole cell proteins increased the surface area of the nanoscale particle by reducing the size of agglomerates leading to increased breakdown of H_2O_2. L-ascorbic acid acts as an anti-oxidant and is able to effectively reduce Fe(III) to Fe(II) in the ratio of 1 mol ascorbic acid per 2 mol Fe(III) at pH < 5 and have slower kinetics when the pH shifts towards alkaline conditions [20]. Cellular proteins are a mixture of simple and conjugated proteins with/without enzymatic functionality. Therefore, from our study we conclude that both ascorbic acid and proteins can be stated to act as capping agents for the α-Fe_2O_3 nano- and microparticles by modifying the surface properties of the particles. The type of interaction between the L-ascorbic acid and proteins with the surface of the α-Fe_2O_3 nano- and microparticles must be further investigated to answer if the particles catalyzed the reduction of H_2O_2 on their surface directly or indirectly by providing space for the L-ascorbic acid and proteins to react with H_2O_2.

In our study, transmission electron microscopy showed an active uptake of the α-Fe_2O_3 nano- and microparticles by human lung cells as large agglomerates. Similar to our observations, Cho et al. [21] have shown that nanoparticles form clusters following agglomeration and reach the cells through sedimentation and diffusion.

Cyto- and genotoxicity studies revealed that both the α-Fe_2O_3 nano- and microscale particles have the ability to induce cyto- and genotoxicity in human lung cells (BEAS-2B and IMR90) *in vitro*. In IMR90-cells the results of genotoxicity analysis were more pronounced after NP-exposure. However, very high particle concentrations of $\geq$ 50 µg/cm² were needed to detect a cellular effect.

The results of the present study also point towards the relationship between loss of cell viability, DNA damage and generation of ROS. Interestingly, the response of the BEAS-2B cells to the α-Fe_2O_3 nanoscale particles regarding ROS formation was delayed by several hours compared to

microparticles. Delayed generation of intracellular ROS can be related to the accumulation of nanoscale particles in large agglomerates after uptake and their fragmentation into smaller ones with increased surface area inside the endoplasmic reticulum (ER).

The physiological role of mitochondria in the generation of oxidative stress and apoptosis is well established [14, 22]. Our study showed an increase in the mitochondrial membrane potential directly proportional to the increasing concentration of the α-Fe_2O_3 nano- and microscale particles. O'Rouke [23] and Nicholls [24] have reported that a high mitochondrial membrane potential indicates an increase in the protonmotive force, thereby increasing the rate of oxidative phosphorylation, K^+ ionophore activation and ROS generation.

In summary, the study indicates that the surface charge and area of α-Fe_2O_3 nano- and microparticles are important for their toxicity to human lung cells. The immediate environment of the particles (presence of biomolecules, chemical composition and physiological properties of the liquid in which they are suspended) modulates their toxicity on the basis of agglomeration rather than their actual size. Nanoparticles showed higher agglomeration in the present study than the microscale particles. The mechanism of toxicity was found to be through the generation of reactive oxygen species (ROS) which itself was modulated by the availability of free surface area. However, the particle concentrations which induced cytotoxicity and DNA damage ($\geq$ 50 µg/ml) are, even in occupational settings, not relevant. At relevant particle concentrations of < 10 µg/ml no DNA breakage can be observed. More sensitive test methods have to be applied here to detect cellular responses caused by nanoparticles.

Acknowledgement

We sincerely thank our technical staff, Mrs. Zimmer and Mrs. Zimmermann whose help and support made the study easy and accompliand within time. We would also like to sincerely thank, Professor Albert W. Rettenmeier, Director, Institute of Hygiene and Occupational Medicine, University Hospital Essen, for his help and support, and Professor Matthias Epple, Department of Inorganic Chemistry, University Duisburg-Essen, Germany for permitting and providing us with the facility of scanning electron microscopy. A part of this work was also conducted under the framework of the INSPIRE programme, funded by the Irish Government's

Programme for Research in Third Level Institutions, Cycle 4, National Development Plan 2007–2013, supported by the European Union Structural Fund.

References

1. OECD *List of manufactured nanomaterials and list of endpoints for phase one of the sponsorship programme for the testing of manufactured nanomaterials: Revision*; Organisation for Economic Co-operation and Development: Paris, 01.12.10, 2010; pp 1-16.
2. Kumar, A.; Sahoo, B.; Montpetit, A.; Behera, S.; Lockey, R. F.; Mohapatra, S. S., Development of hyaluronic acid-Fe2O3 hybrid magnetic nanoparticles for targeted delivery of peptides. *Nanomedicine* **2007,** *3*, (2), 132-7.
3. Zhu, M. T.; Feng, W. Y.; Wang, B.; Wang, T. C.; Gu, Y. Q.; Wang, M.; Wang, Y.; Ouyang, H.; Zhao, Y. L.; Chai, Z. F., Comparative study of pulmonary responses to nano- and submicron-sized ferric oxide in rats. *Toxicology* **2008,** *247*, (2-3), 102-11.
4. Wang, L.; Wang, L.; Ding, W.; Zhang, F., Acute toxicity of ferric oxide and zinc oxide nanoparticles in rats. *J Nanosci Nanotechnol* **2010,** *10*, (12), 8617-24.
5. Wang, B.; Feng, W. Y.; Wang, M.; Shi, J. W.; Zhang, F.; Ouyang, H.; Zhao, Y. L.; Chai, Z. F.; Huang, Y. Y.; Xie, Y. N.; Wang, H. F.; Wang, J., Transport of intranasally instilled Fe2O3 particles into the brain: micro-distribution, chemical states, and histopathological observation. *Biol Trace Elem Res* **2007,** *118*, (3), 233-43.
6. Bhattacharya, K.; Davoren, M.; Boertz, J.; Schins, R. P.; Hoffmann, E.; Dopp, E., Titanium dioxide nanoparticles induce oxidative stress and DNA-adduct formation but not DNA-breakage in human lung cells. *Part Fibre Toxicol* **2009,** *6*, 17.
7. Gramowski, A.; Flossdorf, J.; Bhattacharya, K.; Jonas, L.; Lantow, M.; Rahman, Q.; Schiffmann, D.; Weiss, D. G.; Dopp, E., Nanoparticles Induce Changes of the Electrical Activity of Neuronal Networks on Microelectrode Array Neurochips. *Environ Health Perspect* **2010**.
8. Mahmoudi, M.; Simchi, A.; Milani, A. S.; Stroeve, P., Cell toxicity of superparamagnetic iron oxide nanoparticles. *J Colloid Interface Sci* **2009,** *336*, (2), 510-8.
9. Nel, A. E.; Madler, L.; Velegol, D.; Xia, T.; Hoek, E. M.; Somasundaran, P.; Klaessig, F.; Castranova, V.; Thompson, M., Understanding biophysicochemical interactions at the nano-bio interface. *Nat Mater* **2009,** *8*, (7), 543-57.
10. Lynch, I.; Cedervall, T.; Lundqvist, M.; Cabaleiro-Lago, C.; Linse, S.; Dawson, K. A., The nanoparticle-protein complex as a biological entity; a complex fluids and surface science challenge for the 21st century. *Adv Colloid Interface Sci* **2007,** *134-135*, 167-74.
11. Smoluchowski, M., *Handbuch der Electrizität und des Magnetismus (Graetz)*. Barth: Leipzig, Germany, **1921**; Vol. II, p 366.
12. Beleford, D.; Rattan, R.; Chien, J.; Shridha, V.; High temperature requirement A3(HtrA3) promotes Etoposide- and Cisplatin-induced cytotoxicity in lung cancer cell lines, *Journal of Biological Chemistry* **2010**; 285(16):12011-27.
13. Stang, A.; Witte, I., Performance of comet assay in a high-throughput version. *Mutation research* **2009**; 675(1-2):5-10.
14. Rosado-Berrios, C.A.; Velez, C.; Zayas B., Mitochondrial permeability and toxicity of diethylhexyl and monoethylhexyl phthalates on TK6 human lymphoblasts cells. *Toxicology In vitro*, **2011**; In Press.
15. Donner, M.; Tran, L.; Muller, J.; Vrijhof, H., Genotoxicity of engineered nanomaterials. *Nanotoxicology* **2010**, *4*, 345-6.
16. Cedervall, T.; Lynch, I.; Lindman, S.; Berggard, T.; Thulin, E.; Nilsson, H.; Dawson, K. A.; Linse, S., Understanding the nanoparticle-protein corona using methods to quantify

exchange rates and affinities of proteins for nanoparticles. *Proc Natl Acad Sci U S A* **2007**; *104*, (7), 2050-5.
17. Lundqvist, M.; Stigler, J.; Elia, G.; Lynch, I.; Cedervall, T.; Dawson, K. A., Nanoparticle size and surface properties determine the protein corona with possible implications for biological impacts. *Proc Natl Acad Sci U S A* **2008**; *105*, (38), 14265-70.
18. Bartz, R. R.; Piantadosi, C. A., Clinical review: oxygen as a signaling molecule. *Crit Care* **2010**; *14*(5), 234.
19. Zhou, M.; Yu, Q.; Lei, L.; Barton, G., Electro-Fenton method for the removal of methyl red in an efficient electrochemical system. *Separation and Purification Technology* **2007**; *57*, 380 - 387.
20. Hsieh, Y.-H. P.; Hsieh, Y. P., Valence State of Iron in the Presence of Ascorbic Acid and Ethylenediaminetetraacetic Acid. *J. Agric. Food Chem.* **1997,** *45*, 1126-1129.
21. Cho, E.C.; Zhang, Q.; Xia, Y., The effect of sedimentation and diffusion on the cellular uptake of gold nanoparticles. *Nature Nanotech* **2011**; 6: 385 – 391.
22. Thannickal, V.J.; Fanburg, B.L., Reactive oxygen species in cell signaling. *Am J of Lung Cell Mol Physiol* **2000**; 279(6): L1005-28.
23. O'Rourke, B., Mitochondrial ion channels. *Annu Rev Physiol* **2007**; 69:19-49.
24. Nicholls, D.G., The effective proton conductance of the inner membrane of mitochondria from brown adipose tissue. Dependency on proton electrochemical potential gradient. *European journal of biochemistry / FEBS* **1977**; 77(2):349-356.

a) **b)**

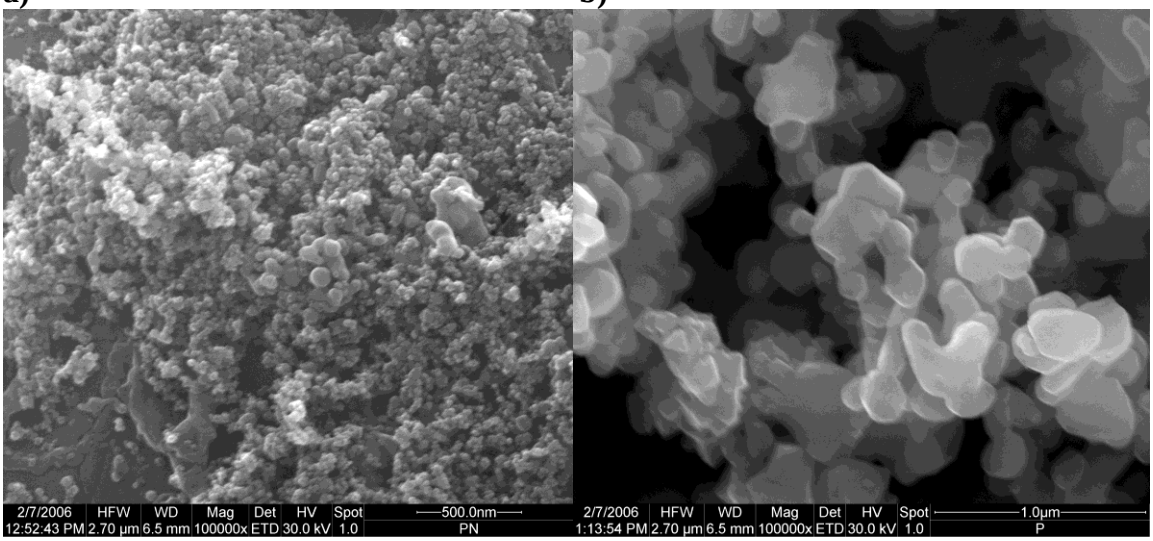

Figure 1: Scanning electron microscopy images of Fe_2O_3 **(a)** nano- and **(b)** microscale particles.

		Zeta potential (mV)	Particle size distribution (Number %; diameter in nm)	Polydispersity Index
Nanoscale particle	**MilliQ Water**	-30.4 ± 0.0	750.7 ± 73.4	0.7 ± 0.1
	Cell Lysate Protein	-25.5 ± 0.6	462 ± 85	1 ± 0.0
	DKSFM + 0.1% Epithelial Growth Factor Protein	-9.35 ± 0.5	776.1 ± 96.4	0.8 ± 0.1
Microscale particle	**MilliQ Water**	-23 ± 0.0	382.1 ± 8.5	0.9 ± 0.1
	Cell Lysate Protein	-30 ± 0.5	171 ± 20.6	1 ± 0.0
	DKSFM + 0.1% Epithelial Growth Factor Protein	-11.1 ± 0.9	347.2 ± 56.0	1 ± 0.0

Table 1: Observed zeta potential (mV), particle size distribution (Number %; diameter in nm) and polydispersity index of α-Fe_2O_3 nano- and microscale particles (concentration: 100 µg/ml) suspended in MilliQ water, cell lysate protein and defined keratinocyte serum free medium (DKSFM) + 0.1% epithelial growth factor protein.

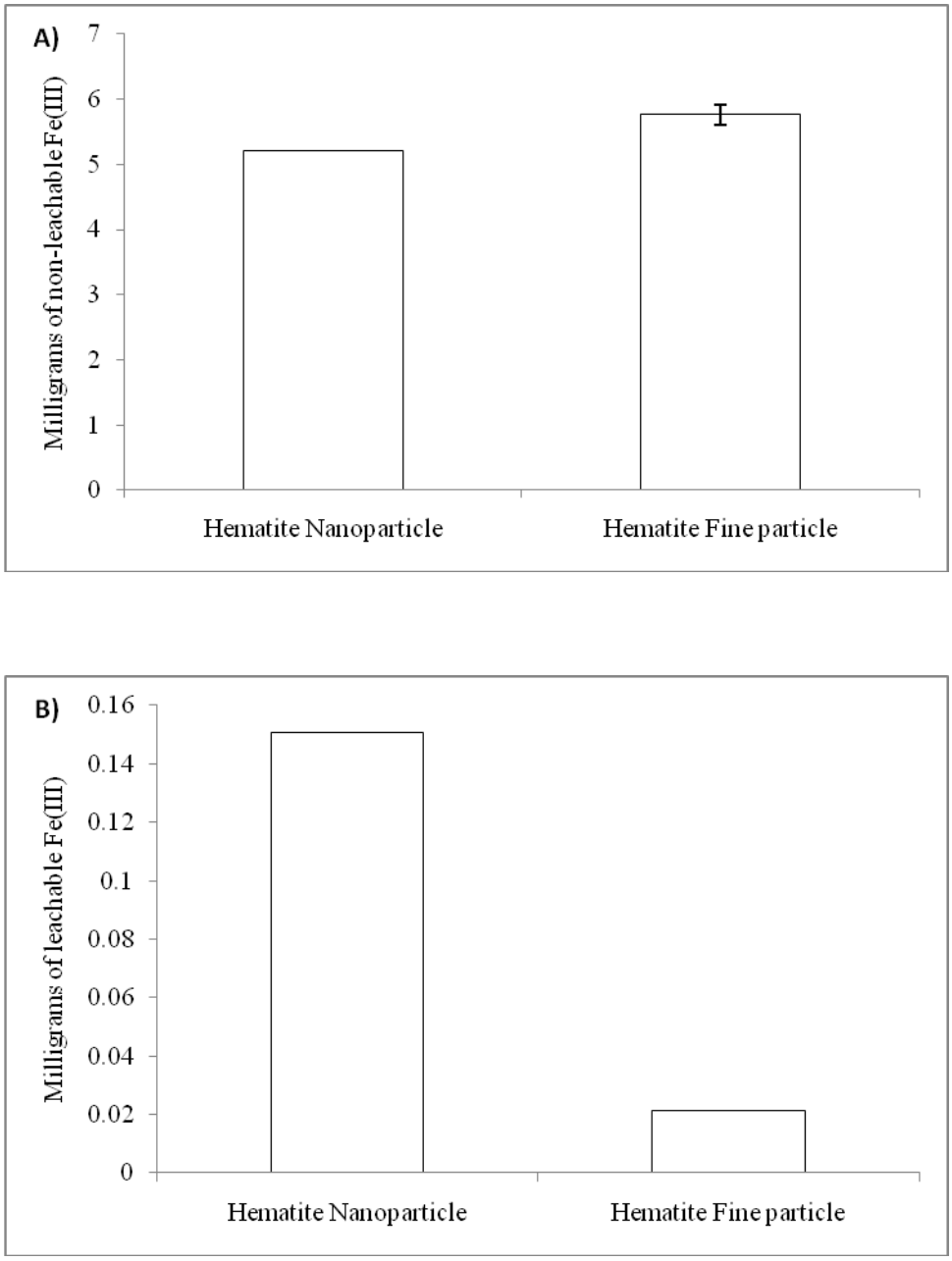

Figure 2: 1,10-Phenanthroline-chloride spectroscopy-based determination of non-leachable **(A)** and leachable Fe(III) **(B)** in Fe_2O_3 nano- and microscale particles. Fe(III) concentrations determined using standard curve of Fe_2Cl_3.

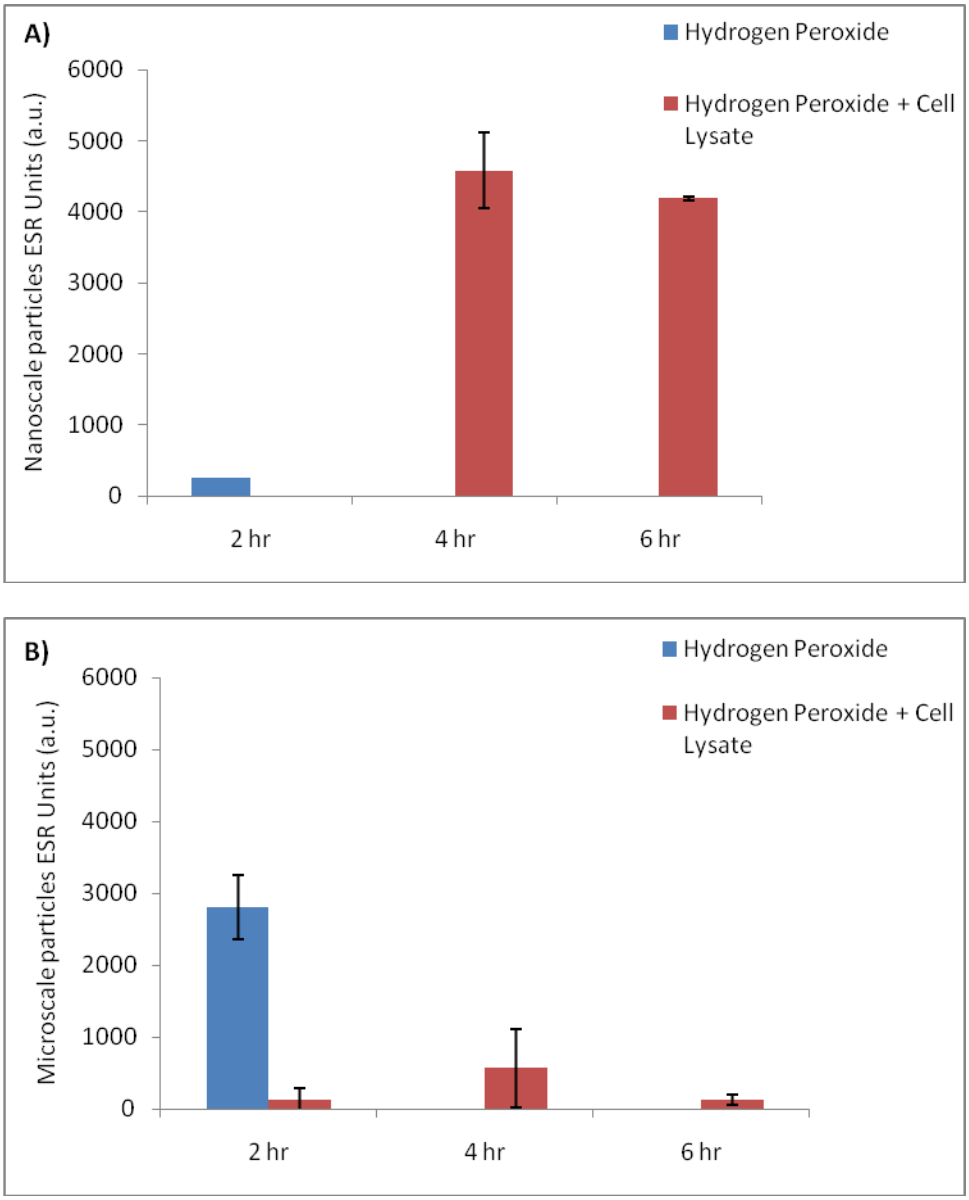

Figure 3: Acellular hydroxyl radical measurement on the surface of α-Fe_2O_3 nano- **(A)** and microscale particles **(B)** using spin trap, 5, 5-dimethyl-1-pyrroline-N-oxide with electron spin resonance (ESR) spectrometry. The particles were suspended in MilliQ water and cell lysate proteins (450 µg/ml) along with hydrogen peroxide (120 mM) treatment. The measurements were taken at time points of 2, 4 and 6 h post-suspension.

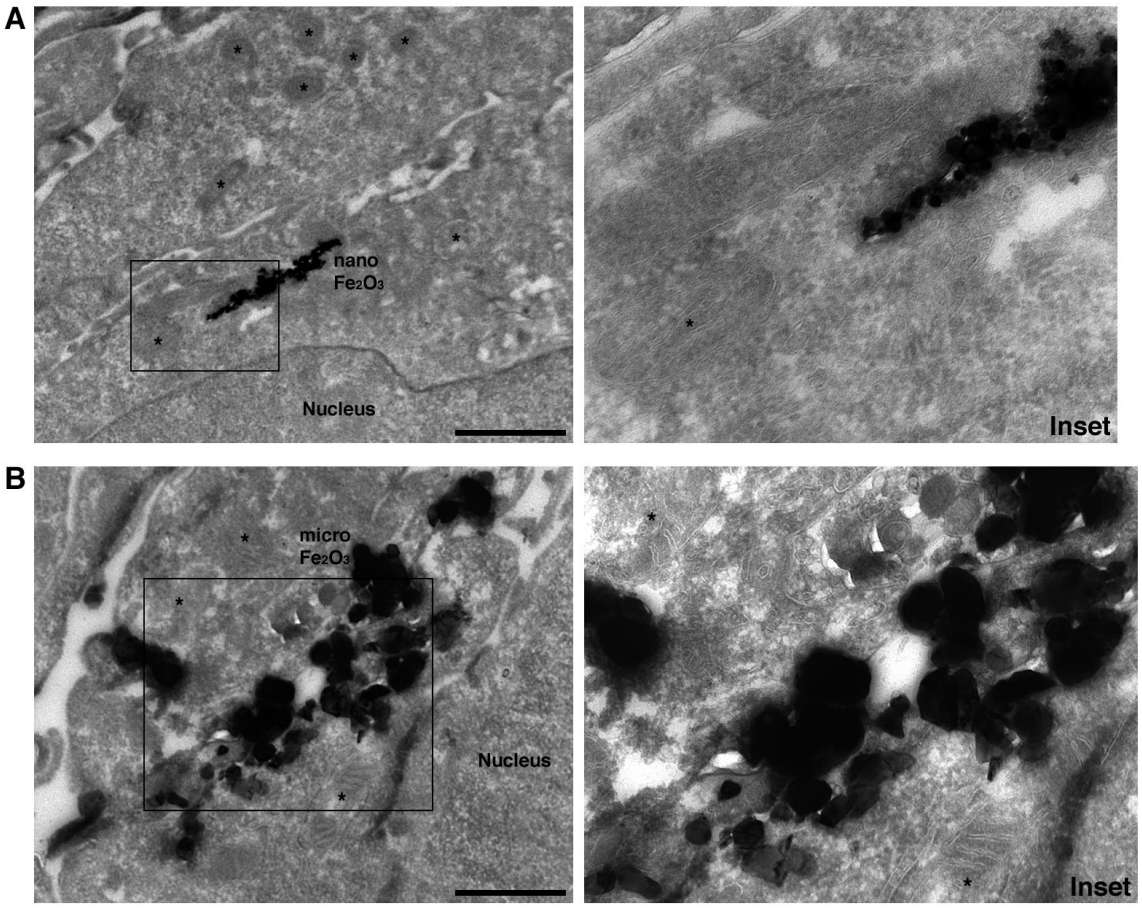

Figure 4: Transmission electron microscopy images of BEAS-2B cells after exposure to 50 µg/ml of α-Fe_2O_3 (A) nanoscale particles and (B) microscale particles for 48 h, respectively. Shown are surrounding mitochondria (*). Bars, 1 µm.

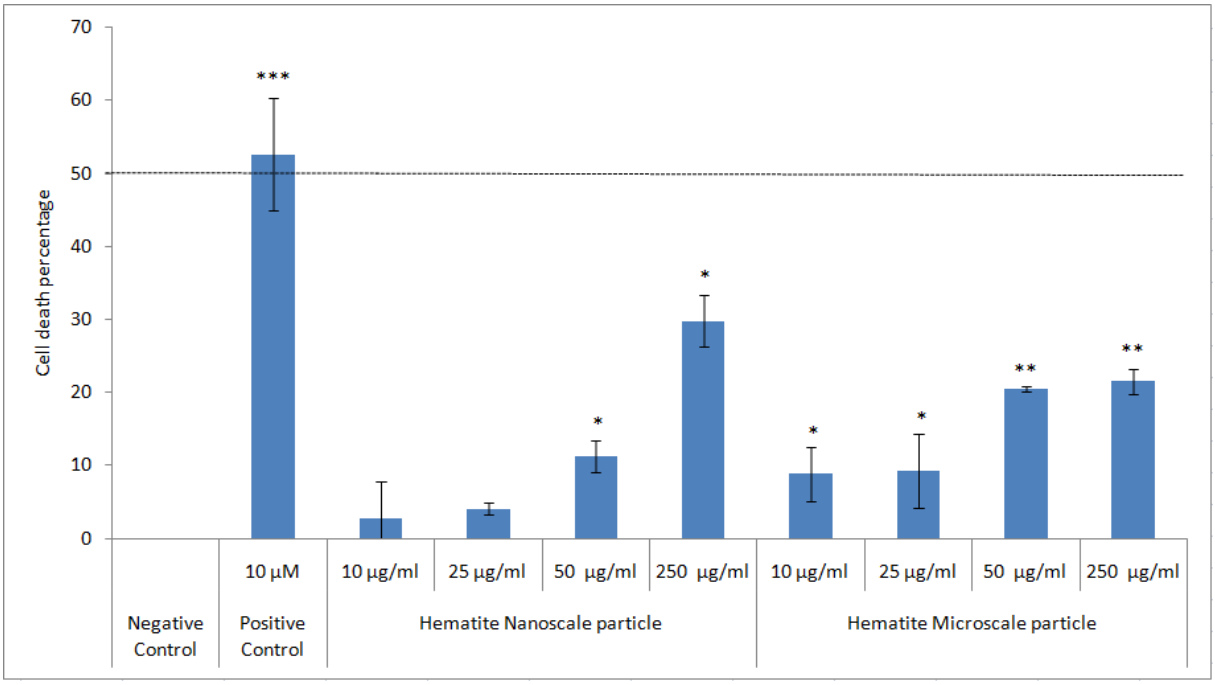

Figure 5: Cytotoxicity in BEAS-2B cells exposed to different concentrations of α-Fe_2O_3 nano- and microscale particles and 10 µM cisplatin (positive control) for 24 h (negative control: without exposure). Values of negative control were set at 0%. P value: * ≤0.05, ** ≤0.01; *** ≤0.001

(A)

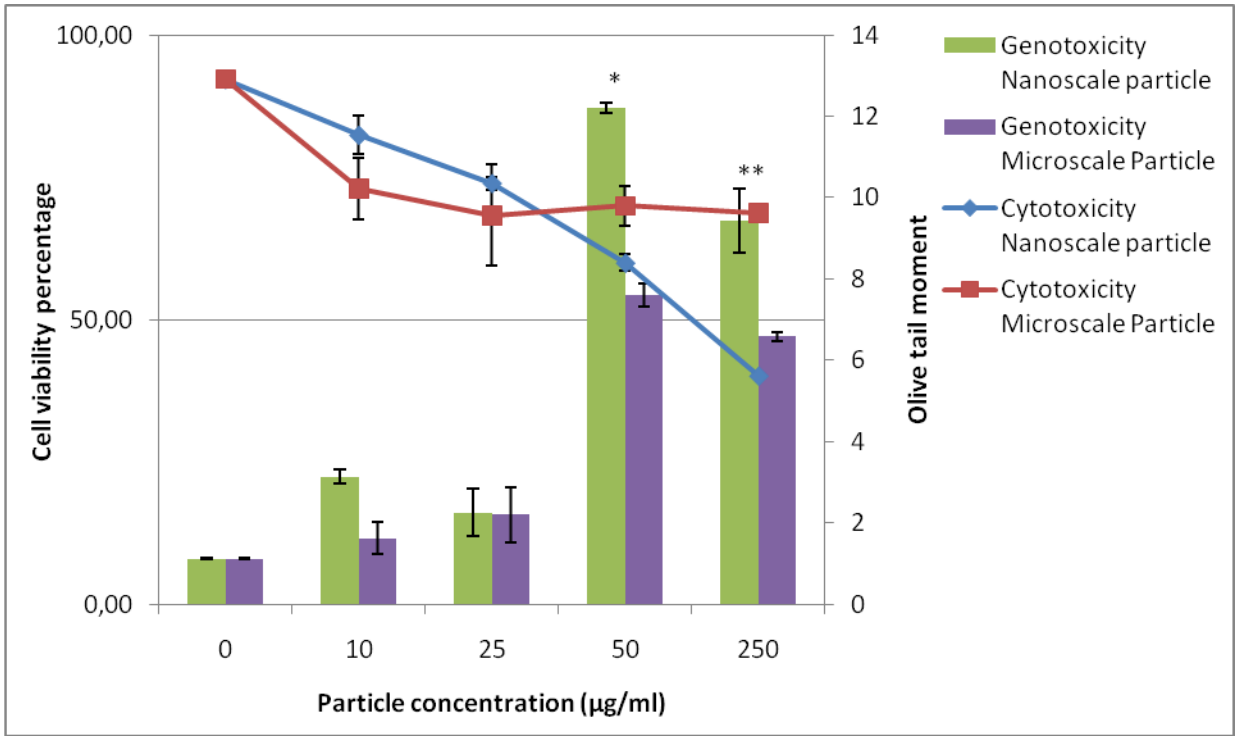
100,00
50,00
0,00
Cell viability percentage
14
12
10
8
6
4
2
0
Olive tail moment
*
**
0
10
25
50
250
Particle concentration (µg/ml)
Genotoxicity Nanoscale particle
Genotoxicity Microscale Particle
Cytotoxicity Nanoscale particle
Cytotoxicity Microscale Particle

B)

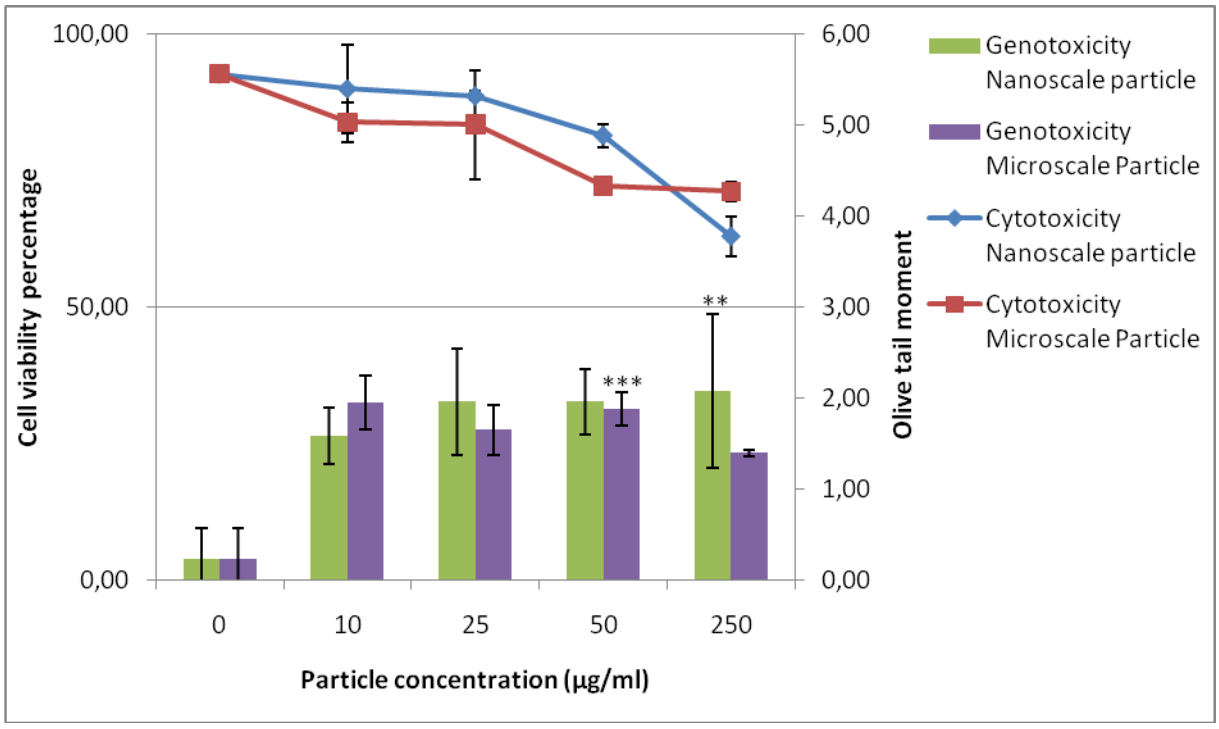
100,00
50,00
0,00
Cell viability percentage
6,00
5,00
4,00
3,00
2,00
1,00
0,00
Olive tail moment
**
***
0
10
25
50
250
Particle concentration (µg/ml)
Genotoxicity Nanoscale particle
Genotoxicity Microscale Particle
Cytotoxicity Nanoscale particle
Cytotoxicity Microscale Particle

Figure 6: Genotoxicity (Comet Assay: Olive tail moment) in **A)** IMR-90 and **B)** BEAS-2B cells following exposure to different concentrations of Fe_2O_3 nano- and microscale particles for 24 h. P value: * ≤0.05, ** ≤0.01; *** ≤0.001. As a negative control cells were exposed to cell culture medium only and as a positive control 200 µM N-ethyl-N-nitrosourea (ENU) was used (OTM in BEAS-2B: 1.5±0.8; in IMR90: 5.8±1.2). P value: * ≤0.05, ** ≤0.01; *** ≤0.001

A)

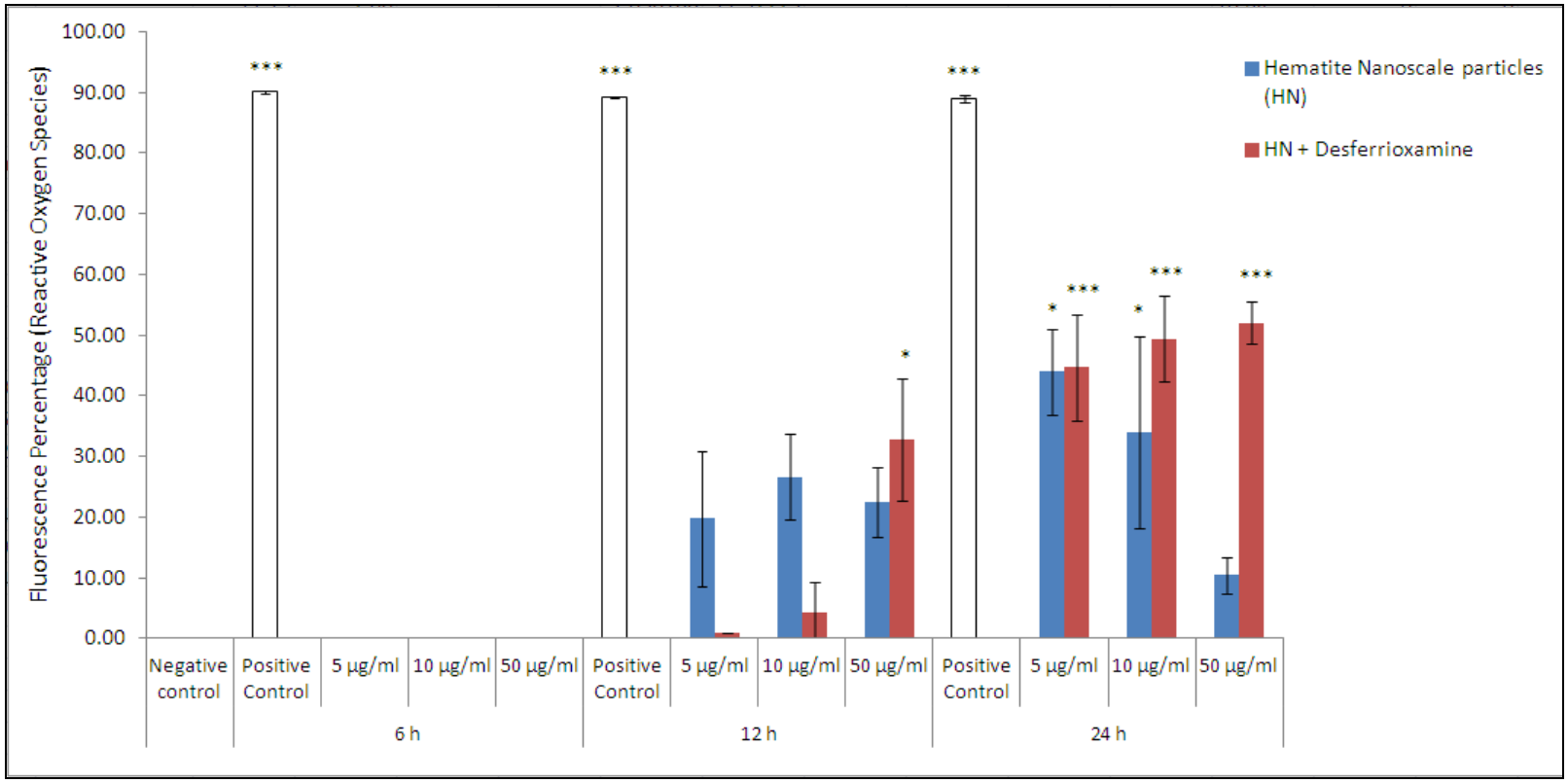
Fluorescence Percentage (Reactive Oxygen Species)
100.00
90.00
80.00
70.00
60.00
50.00
40.00
30.00
20.00
10.00
0.00
Hematite Nanoscale particles (HN)
HN + Desferrioxamine
Negative control
Positive Control
5 µg/ml
10 µg/ml
50 µg/ml
Positive Control
5 µg/ml
10 µg/ml
50 µg/ml
Positive Control
5 µg/ml
10 µg/ml
50 µg/ml
6 h
12 h
24 h

B)

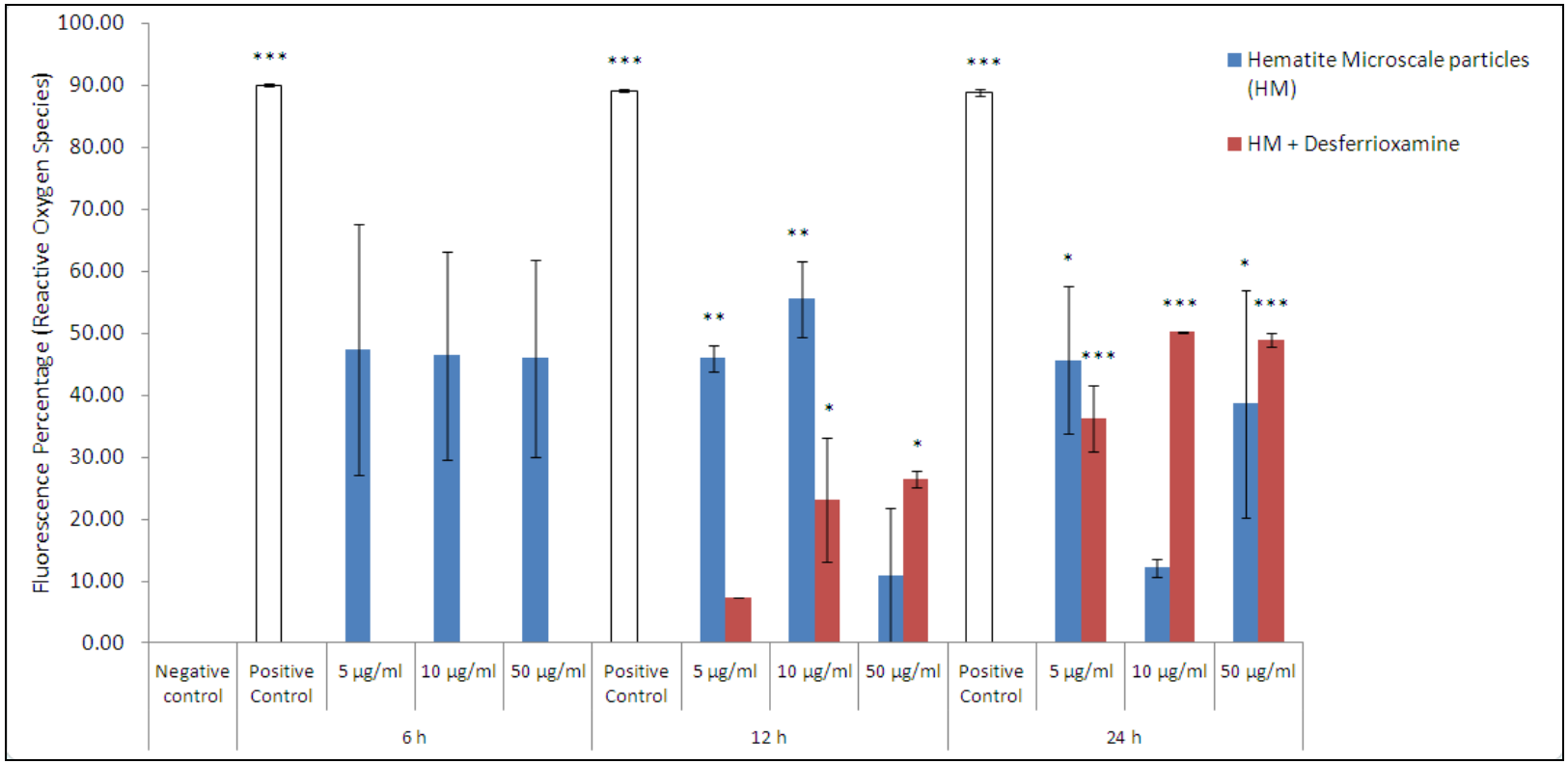

Figure 7: Intracellular reactive oxygen species generation in BEAS-2B cells following exposure to different concentration of **(A)** α-Fe_2O_3 nanoscale particles and **(B)** α-Fe_2O_3 microscale particles with and without addition of the iron chelator siderophore Desferrioxamine mesylate (100 µg/ml). The nano- and microscale particle concentrations were 5, 10 and 50 µg/ml. Cells were exposed for the time periods of 6, 12 and 24 h. As negative control, culture medium and as positive control 10 µM Cisplatin was used (p value ≤0.05 *; ≤0.01 **; ≤0.001 ***). Negative control was set as 0%.

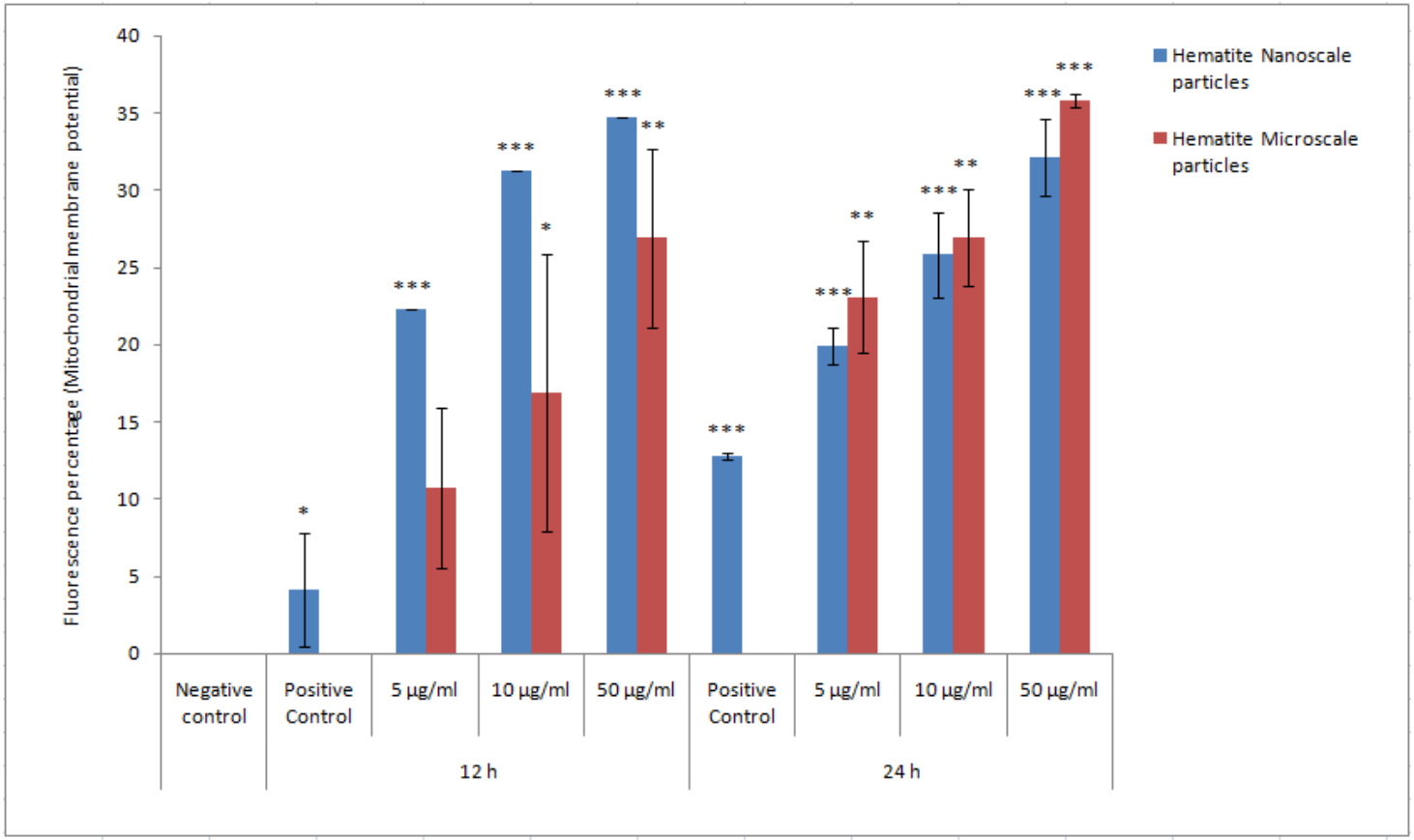

Figure 8: Mitochondrial membrane potential of the BEAS-2B cells after exposure to different concentration of Fe_2O_3 nano- and microscale particles at concentrations of 5, 10 and 50 µg/ml (exposure time: 12 and 24 h). As negative control, cells were exposed to only cell culture medium and as positive control to 100 µM of Valinomycin. (P value ≤0.05 *; ≤0.01 **; ≤0.001 ***). Negative control was set as 0%.